

A new quark-hadron hybrid equation of state for astrophysics

I. High-mass twin compact stars

Sanjin Benić^{1,2} *, David Blaschke^{3,4} **, David E. Alvarez-Castillo^{4,5} ***, Tobias Fischer³ †, and Stefan Typel⁶ ‡

¹ Physics Department, Faculty of Science, University of Zagreb, Bijenička c. 32, Zagreb 10000, Croatia

² Department of Physics, The University of Tokyo, 7-3-1 Hongo, Bunkyo-ku, Tokyo 113-0033, Japan

³ Institute for Theoretical Physics, University of Wrocław, Pl. M. Borna 9, 50-204 Wrocław, Poland

⁴ Bogoliubov Laboratory for Theoretical Physics, Joint Institute for Nuclear Research, 141980 Dubna, Russia

⁵ Instituto de Física, Universidad Autónoma de San Luis Potosí, S.L.P. 78290, México

⁶ GSI Helmholtzzentrum für Schwerionenforschung GmbH, Planckstraße 1, 64291 Darmstadt, Germany

Received: day month year; accepted: day month year

ABSTRACT

Aims. We present a new microscopic hadron-quark hybrid equation of state model for astrophysical applications, from which compact hybrid star configurations are constructed. These are composed of a quark core and a hadronic shell with first-order phase transition at their interface. The resulting mass-radius relations are in accordance with the latest astrophysical constraints.

Methods. The quark matter description is based on a QCD motivated chiral approach with higher-order quark interactions in the Dirac scalar and vector coupling channels. For hadronic matter we select a relativistic mean-field equation of state with density-dependent couplings. Since the nucleons are treated in the quasi-particle framework, an excluded volume correction has been included for the nuclear equation of state at suprasaturation density which takes into account the finite size of the nucleons.

Results. These novel aspects, excluded volume in the hadronic phase and the higher-order repulsive interactions in the quark phase, lead to a strong first-order phase transition with large latent heat, i.e. the energy-density jump at the phase transition, which fulfills a criterion for a disconnected third-family branch of compact stars in the mass-radius relationship. These *twin* stars appear at high masses ($\sim 2 M_{\odot}$) being relevant for current observations of high-mass pulsars.

Conclusions. This analysis offers a unique possibility by radius observations of compact stars to probe the QCD phase diagram at zero temperature and large chemical potential and even to support the existence of a critical point in the QCD phase diagram.

Key words. stars: neutron – stars: interiors – dense matter – equation of state

1. Introduction

The physics of compact stars is an active subject of modern nuclear astrophysics research since it allows to probe the state of matter at conditions which are currently inaccessible in high-energy collider facilities: extremes of baryon density at low temperature. It provides one of the strongest observational constraints on the zero-temperature equation of state (EoS) by recent high-precision mass measurement of high-mass pulsars by Demorest et al. (2010) and Antoniadis et al. (2013). Any scenarios for the existence of exotic matter and a phase transition at high density which tend to soften the EoS may be abandoned unless they provide stable compact star configurations with a mass not less than $2 M_{\odot}$. Still, there are several possibilities for which it is hard or impossible to detect quark matter in compact stars, namely when: a) the phase transition occurs at too high densities, exceeding the central density of the maximum mass configuration, b) the transition occurs only very close to the maximum mass, beyond the limit of masses for observed high-mass pulsars, or when c) the transition is a crossover or very close to it so that the hybrid star characteristics is indistinguishable from that

of pure neutron stars. The latter case has been dubbed “masquerade” problem Alford et al. (2005). The latter case seems to be characteristic to the use of modern chiral quark models with vector meson interactions Bratovic et al. (2013) which are very similar in their behaviour to standard nuclear EoS like APR (Akmal, Pandharipande & Ravenhall, 1998) or DBHF (Fuchs, 2006) in the transition region (see, e.g., Klähn et al. (2007), Klähn et al. (2013)). However, the opposite case is also possible: when the phase transition to quark matter is accompanied with a large enough binding energy release, corresponding to a jump in density and thus a compactification of the star, an instability may be triggered which eventually will result in the emergence of a third family of compact stellar objects, in addition of white dwarfs and neutron stars. About the existence of such a branch of supercompact stellar objects which is *disconnected* from the neutron star sequence has long been speculated in different context related to phase transitions in dense matter (c.f. Gerlach, 1968; Kämpfer, 1981; Schertler et al., 2000; Glendenning & Kettner, 2000). This phenomenon has been studied due to the appearance of pion and kaon condensates in Kämpfer (1981) and Banik & Bandyopadhyay (2001) respectively, as well as hyperons in Schaffner-Bielich et al. (2002) and quark matter in Glendenning & Kettner (2000), Schertler et al. (2000), Fraga et al. (2002), Banik & Bandyopadhyay (2003), Agrawal & Dhiman (2009), and Agrawal (2010). All these early studies, however, could be ruled out by the recent observa-

* e-mail: sanjinb@phy.hr

** e-mail: blaschke@ift.uni.wroc.pl

*** e-mail: alvarez@theor.jinr.ru

† e-mail: fischer@ift.uni.wroc.pl

‡ e-mail: s.typel@gsi.de

tion of high-mass pulsars. The question arose whether the twin star phenomenon as an indicator for a first order phase transition could also concern compact stars with masses as high as $2 M_{\odot}$. If answered positively, the observation of significantly different radii for high-mass pulsars of the same mass would allow conclusions also for isospin symmetric matter as probed in heavy-ion collisions.

The ongoing heavy-ion programs at the collider facilities at RHIC (US) and LHC at CERN in Geneva (Switzerland), combined with the success of modern lattice QCD, did lead to the result that the nature of the QCD transition at vanishing chemical potential and finite temperature is a crossover. The physics of the QCD phase diagram at finite chemical potential and finite temperatures will be subject of research within the future high-energy facilities at FAIR in Darmstadt (Germany) and NICA in Dubna (Russia) where one of the main goals is to find a critical endpoint (CEP) of first-order transitions or, indications for a first order phase transition at high baryon density like signatures for a quark-hadron mixed phase. In general, a phase transition in isospin asymmetric stellar matter is directly related to the corresponding phase transition in symmetric matter, and therefore relevant to the understanding of the QCD phase diagram (c.f. Fukushima & Sasaki, 2013; Fukushima, 2014). Since increasing the isospin asymmetry would result in lowering the temperature of the CEP to zero (Ohnishi et al., 2011) the detection of first order phase transition signals in zero temperature asymmetric compact star matter like the mass twin phenomenon would thus prove the existence of at least one CEP in the QCD phase diagram Alvarez-Castillo & Blaschke (2013); Blaschke et al. (2013).

The major ingredient of compact star physics is the zero-temperature EoS in β -equilibrium (for recent works, c.f. Steiner et al., 2013; Masuda et al., 2013; Orsaria et al., 2013; Alford et al., 2013; Hebeler et al., 2013; Inoue et al., 2013; Klähn et al., 2013; Fraga et al., 2013; Yasutake et al., 2014; Yamamoto et al., 2014). More precisely, hybrid EoS can be decomposed into three parts: (a) low-density nuclear matter, (b) high-density *exotic* matter such as hyperons or quarks, (c) the phase transition region between low- and high-density parts. The conditions for the transition depend on details of the underlying microscopic descriptions of matter. For the EoS to yield a third family and/or the twin phenomenon, the following two conditions should be fulfilled (for details, see Haensel et al., 2007; Read et al., 2009; Zdunik & Haensel, 2013; Alford et al., 2013):

(1) The latent heat of the phase transition should fulfill a constraint $\Delta\varepsilon > \Delta\varepsilon_{\min}$ (Haensel et al., 2007; Zdunik & Haensel, 2013; Alford et al., 2013) where $\Delta\varepsilon_{\min} \sim 0.6\varepsilon_{\text{crit}}$ for the schematic hybrid EoS investigated in (Alford et al., 2013) and (Alvarez-Castillo & Blaschke, 2013) with $\varepsilon_{\text{crit}}$ being the critical energy density for the onset of the transition.

(2) The high density part of the EoS should be sufficiently stiff.

The third family of compact objects is attained via an unstable branch, which can be realized by a soft EoS in the transition region, ensured by the condition (1). The condition (2) is necessary for the core matter to withstand the pressure from the hadronic shell and thus to provide stability for the new, disconnected hybrid star branch.

Confirming the existence of high-mass twins represents an outstanding challenge for observational campaigns to develop precise radius measurements for compact stellar objects (c.f.

Mignani et al., 2012; Gendreau et al., 2012; Miller, 2013). If detected, the twin phenomenon would be a compelling astrophysical signature of a strong first-order phase transition in the QCD phase diagram at zero temperature and thus strong evidence for the presence of at least one critical end point. By invoking that the high-mass pulsars PSR J1614-2230 by Demorest et al. (2010) and PSR J0348+0432 Antoniadis et al. (2013), with their precisely measured masses $1.97 \pm 0.04 M_{\odot}$ and $2.01 \pm 0.04 M_{\odot}$, respectively, could be such twin stars, we predict in this work that their radii should differ at least by about 1 km (depending on the model details). It remains to be shown whether these values are within the capabilities of future experimental X-ray satellite missions like the Neutron Star Interior Composition Explorer (NICER)¹, the Nuclear Spectroscopic Telescope Array (NUSTAR)² and/or the Square Kilometer Array (SKA)³.

In this work we present a microscopically founded example for the class of hybrid EoS that fulfill the criteria (1), (2) for the occurrence of a third family of compact stars based on a first-order phase transition from hadronic matter to quark matter. In our case, the nuclear matter phase is described by a relativistic mean-field (RMF) model with density-dependent meson-nucleon couplings introduced in Typel & Wolter (1999) using the DD2 parametrization from Typel et al. (2010) with finite-volume modifications. The quark matter phase is given by a Nambu-Jona-Lasinio model (NJL) with higher-order quark interactions, as introduced in Benić (2014). For the phase transition between hadronic and quark matter phases we apply a Maxwell construction. The resulting quark-hadron hybrid EoS allows for massive twin star configurations for which their gravitational masses are in agreement with the present $2 M_{\odot}$ constraint set by Demorest et al. (2010) and Antoniadis et al. (2013).

The paper is organized as follows: in Sect. 2 we introduce our new quark-hadron hybrid EoS and in Sect. 3 we discuss characteristic features of it such as excluded volume, mass-radius relations and twin configurations. The paper closes with the summary in Sect. 4.

2. Model Equation of State for massive twin phenomenon

For quark matter at high densities we employ the recently proposed NJL-based model of Benić (2014). For the low-density region we use the nuclear RMF EoS (Typel & Wolter, 1999) with the well-calibrated DD2 parametrization of Typel et al. (2010). In order to maximize the latent heat at the phase transition, we correct the standard DD2 EoS by accounting for an excluded volume of the nucleons that results from Pauli blocking due their quark substructure. The latter aspect will be further introduced in the following subsection.

2.1. Excluded nucleon volume in the hadronic Equation of State

The composite nature of nucleons can be modeled by the excluded-volume mechanism as discussed e.g. by (Rischke et al., 1991) in the context of RMF models. Considering nucleons as hard spheres of volume V_{nuc} , the available volume V_{av} for the motion of nucleons is only a

¹ <http://heasarc.gsfc.nasa.gov/docs/nicer/index.html>

² <http://www.nasa.gov/mission-pages/nustar/main>

³ <http://www.skatelescope.org>

fraction $\Phi = V_{av}/V$ of the total volume V of the system. The available volume fraction can be written as

$$\Phi = 1 - v \sum_{i=n,p} n_i , \quad (1)$$

with the nucleon number densities n_i and the volume parameter

$$v = \frac{1}{2} \frac{4\pi}{3} (2r_{\text{nuc}})^3 = 4V_{\text{nuc}} , \quad (2)$$

if we assume identical radii $r_{\text{nuc}} = r_n = r_p$ of neutrons and protons. The total hadronic pressure and energy density are given by the following relations:

$$p_{\text{tot}}(\mu_n, \mu_p) = \frac{1}{\Phi} \sum_{i=n,p} p_i + p_{\text{mes}} , \quad (3)$$

$$\varepsilon_{\text{tot}}(\mu_n, \mu_p) = -p_{\text{tot}} + \sum_{i=n,p} \mu_i n_i , \quad (4)$$

with contributions from nucleons and mesons. They depend on the nucleon chemical potentials μ_n and μ_p . The nucleonic pressures are given by

$$p_i = \frac{1}{4} (E_i n_i - m_i^* n_i^{(s)}) , \quad (5)$$

with the nucleon number densities and scalar densities:

$$n_i = \frac{\Phi}{3\pi^3} k_i^3 , \quad (6)$$

$$n_i^{(s)} = \frac{\Phi m_i^*}{2\pi^2} \left[E_i k_i - (m_i^*)^2 \ln \frac{k_i + E_i}{m_i^*} \right] , \quad (7)$$

that contain the energies

$$E_i = \sqrt{k_i^2 + (m_i^*)^2} = \mu_i - V_i - \frac{v}{\Phi} \sum_{j=p,n} p_j , \quad (8)$$

as well as Fermi momenta k_i and effective masses $m_i^* = m_i - S_i$. The vector potentials V_i , scalar potentials S_i and the mesonic contribution p_{mes} to the total pressure have the usual form of RMF models with density-dependent couplings (for more details, see Typel & Wolter, 1999).

Table 1. Parameters of the DD2-EV model. The definition of the quantities are given in Typel et al. (2010).

meson i	ω	σ	ρ
$\Gamma_i(n_{\text{sat}})$	12.920700	10.826881	2.296878
a_i	1.693762	1.357629	2.215411
b_i	-0.002358	0.634443	-
c_i	0.050349	1.005359	-
d_i	2.573015	0.575809	-

In conventional RMF models the in-medium nucleon-nucleon interaction is modeled by the exchange of (σ , ω and ρ) mesons between pointlike nucleons. The excluded volume causes an additional effective repulsion between the nucleons. Hence, the parameters of the RMF model have to be refitted in order to retain the characteristic properties of nuclear matter. The parameters of the nucleon-meson couplings in the DD2 RMF model were determined by fitting to properties of finite nuclei (for details, see Typel et al., 2010). This approach leads to very

satisfactory results all over the nuclear chart and gives nuclear matter parameters that are consistent with current experimental constraints. In table 1 the parameters of the new parametrization DD2-EV with excluded-volume effects are given assuming a volume parameter $v = (1/0.35) \text{ fm}^3$. This corresponds to a nucleon radius of $r_{\text{nuc}} \approx 0.55 \text{ fm}$. See Typel et al. (2010) for the definition of the quantities in the table and their relation to the coupling functions. The saturation density n_{sat} and the particle masses are not changed as compared to the original DD2 parametrization. The DD2-EV parameters were determined such that the binding energy per nucleon E/A , the compressibility K , the symmetry energy J and the symmetry energy slope parameter L are also identical to that of the DD2 effective interaction.

For the hadronic EoS we use the original DD2 parametrization without excluded-volume effects at baryon densities below the saturation density n_{sat} of the model since these densities are well tested in finite-nucleus calculations. At densities above n_{sat} we replace the DD2 model by the DD2-EV parametrization with excluded-volume corrections. The maximum baryon density that can be described by this model is $n_{\text{max}} = 1/v = 0.35 \text{ fm}^{-3}$ due to the choice of the volume parameter v . At this density the pressure diverges and the transition to quark matter has to occur below n_{max} . In stellar matter the usual contributions to the pressure and energy density of the electrons are added to the hadronic part. Requiring charge neutrality, i.e. $n_e = n_p$ and β equilibrium, i.e. $\mu_n = \mu_p + \mu_e$, the pressure and energy density become functions of a single quantity, the baryon chemical potential $\mu_B = \mu_n$.

2.2. NJL model with 8-quark interactions

In order to describe cold quark matter that is significantly stiffer than the ideal gas, we employ the recently developed generalization of the NJL model by Benić (2014), which includes 8-quark interactions in both, Dirac scalar and vector channels (NJL8). The mean-field thermodynamic potential of the 2-flavor NJL8 model is given as follows:

$$\Omega = U - 2N_c \sum_{f=u,d} \left[\frac{1}{2\pi^2} \int_0^\Lambda dp p^2 E_f - \frac{1}{48\pi^2} \left\{ (2\tilde{\mu}_f^3 - 5M_f^2 \tilde{\mu}_f) \times \sqrt{\tilde{\mu}_f^2 - M_f^2} + 3M_f^4 \ln \left(\frac{\sqrt{\tilde{\mu}_f^2 - M_f^2} + \tilde{\mu}_f}{M_f} \right) \right\} \right] - \Omega_0 , \quad (9)$$

with

$$U = 2 \frac{g_{20}^2}{\Lambda^2} (\phi_u^2 + \phi_d^2) + 12 \frac{g_{40}^2}{\Lambda^8} (\phi_u^2 + \phi_d^2)^2 - 2 \frac{g_{02}^2}{\Lambda^2} (\omega_u^2 + \omega_d^2) - 12 \frac{g_{04}^2}{\Lambda^8} (\omega_u^2 + \omega_d^2)^2 , \quad (10)$$

and energy-momentum relation, $E_f = \sqrt{p^2 + M_f^2}$, with

$$M_u = m + 4 \frac{g_{20}}{\Lambda^2} \phi_u + 16 \frac{g_{40}}{\Lambda^8} \phi_u^3 + 16 \frac{g_{04}}{\Lambda^8} \phi_u \phi_d^2 , \quad (11)$$

$$\tilde{\mu}_u = \mu_u - 4 \frac{g_{02}^2}{\Lambda^2} \omega_u - 16 \frac{g_{04}^2}{\Lambda^8} \omega_u^3 - 16 \frac{g_{04}^2}{\Lambda^8} \omega_u \omega_d^2 . \quad (12)$$

Expressions for M_d and $\tilde{\mu}_d$ are obtained by cyclic permutation of indices in (11) and (12), respectively. The model parameters are the 4-quark scalar and vector couplings g_{20} , and g_{02} , the 8-quark scalar and vector couplings g_{40} and g_{04} as well as the current quark mass m and the momentum cutoff Λ which is placed on the divergent vacuum energy. The constant Ω_0 ensures zero pressure in the vacuum.

The model is solved by means of finding the extremum value of the thermodynamic potential (9) with respect to the mean-fields ($X = \phi_u, \phi_d, \omega_u, \omega_d$), i. e.

$$\frac{\partial \Omega}{\partial X} = 0, \quad (13)$$

and the pressure is obtained from the relation $p = -\Omega$.

In this work we use the parameter set of Kashiwa et. al. (2007), $g_{20} = 2.104$, $g_{40} = 3.069$, $m = 5.5$ MeV and $\Lambda = 631.5$ MeV. Furthermore, the vector channel strengths are quantified by the ratios

$$\eta_2 = \frac{g_{02}}{g_{20}}, \quad \eta_4 = \frac{g_{04}}{g_{40}}. \quad (14)$$

Here, we will concentrate on the parameter space where η_2 is small and use η_4 to control the stiffness of the EoS. Note that small η_2 ensures an early onset of quark matter, i.e. it refers to low densities for the onset of quark matter (depending on the stiffness of the nuclear EoS at corresponding densities).

Within this approach we can calculate the partial pressures p_f and densities $n_f = \partial p_f / \partial \mu_f$ for $f = (u, d)$. In neutron stars, neutrino-less β -equilibrium is typically fulfilled, i.e. the corresponding equilibrium weak process in nuclear matter is the nuclear β -decay: $n \rightleftharpoons p + e^- + \bar{\nu}_e$. In quark matter, it is replaced by: $d \rightleftharpoons u + e^- + \bar{\nu}_e$, and hence here the following relation holds between the contributing chemical potentials, $\mu_d = \mu_u + \mu_e$ (neutrino escapes from the star so his chemical potential is set to zero). Moreover, the following condition,

$$\sum_{i=u,d,e} Z_i n_i = \frac{2n_u}{3} - \frac{n_d}{3} - n_e = 0, \quad (15)$$

ensures local charge neutrality. The total pressure in the quark phase is then given by the sum of the partial pressures, $p = p_u + p_d + p_e$, with electron pressure p_e . The latter is calculated based on the relativistic and degenerate Fermi gas. Moreover, the baryon chemical potential and the baryon density in the quark phase (Q) and hadronic phase (H) are obtained as follows,

$$\mu_B^Q = \mu_u + 2\mu_d, \quad \mu_B^H = \mu_n, \quad (16)$$

$$n_B^Q = \frac{\partial p}{\partial \mu_B^Q} = \frac{n_u + n_d}{3}, \quad n_B^H = n_p + n_n, \quad (17)$$

with neutron and proton chemical potentials (μ_n, μ_p) and densities (n_n, n_p). When no confusion arises indices Q and H will be omitted for simplicity.

For the construction of the phase transition, we apply Maxwell's condition in the pressure-chemical potential plane, i.e. pressures in quark and hadronic phases must be equal $p_H(\mu_B^H) = p_Q(\mu_B^Q)$ at coexistence $\mu_B^H = \mu_B^Q$, in order to ensure thermodynamic consistency. This approach is tantamount to assuming a large surface tension at the hadron-quark interface. The critical baryon chemical potential is obtained by matching the pressures from the hadronic (DD2-EV) and quark (NJL8) EOSs. With this setup, a first-order phase transition is obtained by construction with a significant jump in baryon density and energy density as illustrated in Fig. 1. It will be further discussed in the subsequent Sect. 3.

3. Results

The model parameters used to calculate the hybrid EoS are as follows. We modify the DD2 EoS with the excluded volume mechanism as described in Subsect. 2.1 (DD2-EV). The

high-density part is given by the NJL8 EoS (9), where we use $\eta_2 = 0.08$ and consider η_4 as a free parameter.

The rationale behind our choice of a low value for η_2 and the particular value for ν is at this stage purely phenomenological. The parameter η_2 controls both the onset of quark matter as well as the stiffness of the quark EoS. Note that a measure for the stiffness (or softness) of the EoS is the speed of sound c_s defined via

$$c_s^2 = \frac{\partial p}{\partial \epsilon} = \frac{\partial \ln \mu_B}{\partial \ln n_B}. \quad (18)$$

When comparing two EoS, the stiffer one has the steeper slope of $p(\epsilon)$ while its slope of $n(\mu_B)$ is lower. In the present model, a larger value for η_2 would result in more similar quark and hadronic EoS, and hence disfavor the anticipated condition of maximized latent heat at the phase transition. Incidentally, since a small value of η_2 ensures a low onset of quark matter, the nuclear EoS is insensitive to the detailed behavior of the Φ function close to the maximum density n_{\max} . Thus we use the traditional linear dependence (1) on the nucleon densities.

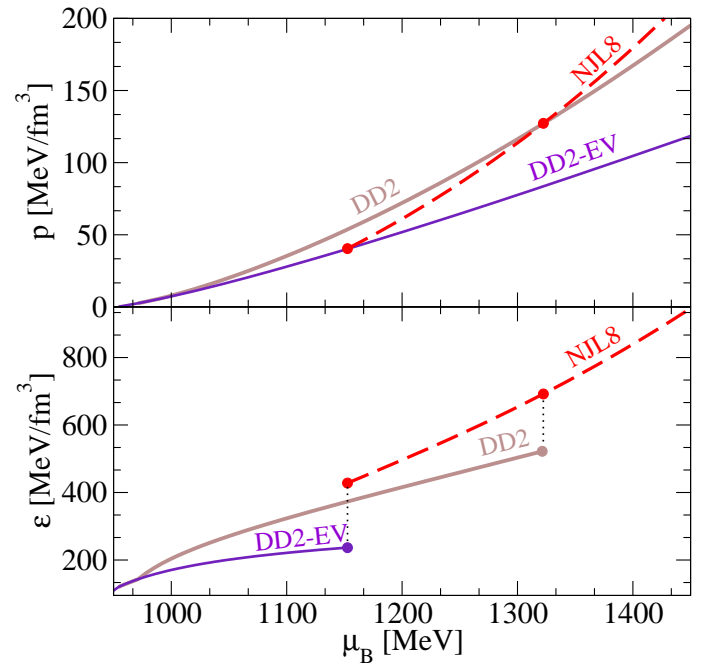


Fig. 1. (Color online) Upper panel: Maxwell construction in the $P - \mu_B$ plane for the DD2 EoS (brown solid line) and the NJL8 EoS (red dashed line) for $\eta_2 = 0.08$, $\eta_4 = 0.0$, as well as the DD2-EV EoS (violet solid line) and the same NJL8 EoS parametrization. Lower panel: the same construction as in the upper panel for the corresponding $\epsilon - \mu_B$ plane.

3.1. Hybrid Equation of State

The new quark-hadron hybrid EoS, based on DD2-EV and NJL8, is shown in the upper panel of Fig. 2 illustrating the pressure-energy density plane, for fixed $\eta_2 = 0.08$ and varying vector-coupling parameters η_4 . Note that with increasing vector coupling parameters, η_2 and η_4 , the sound speed rises which is shown in the lower panel of Fig. 2. Note further that the different dimensionality of the 4-quark and 8-quark vector operators separates the region in density in which the respective operator

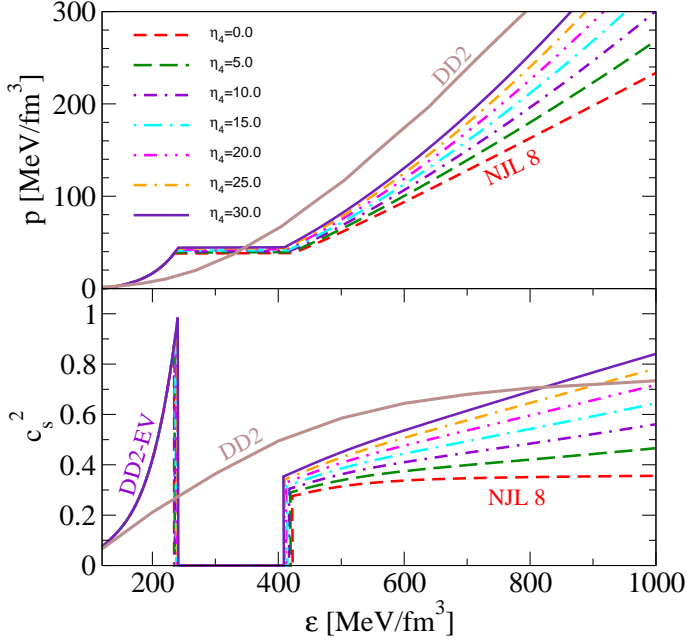


Fig. 2. (Color online) Upper panel: Hybrid EoS built from DD2-EV and NJL8 with phase transition via the Maxwell construction, for the NJL8 parameter $\eta_2 = 0.08$ and varying η_4 from 0.0 – 30. Lower panel: squared speed of sound for these hybrid EoS. For comparison, in both panels the hadronic EoS DD2 is shown (solid brown line).

influences the speed of sound. In particular, while η_2 controls the stiffness of the EoS in the low density region, η_4 stiffens the EoS in the high density region. This can be seen from Fig. 2 where $\eta_2 = 0.08$ and η_4 is varied from $\eta_4 = 0.0$ (red dashed line) to $\eta_4 = 30.0$ (violet solid line). In addition to the selected values shown in Fig. 2, we explored the total parameter range $\eta_4 = 0.0 - 30.0$ in steps of $\Delta\eta_4 = 1.0$. Above the maximum value of $\eta_4 = 30.0$ the transition from DD2-EV to NJL8 violates the requirement of causality, see also Fig. 2, which takes place at $\epsilon \simeq 240 \text{ MeV fm}^{-3}$. We have checked that in all our cases the causality limit is reached only at energy densities beyond which the mass-radius sequences turn unstable.

Exploring the available parameter spaces in both, hadronic and quark matter phases, we have found the maximized latent heat in the combination of two aspects: (a) taking into account finite-size effects of the nucleons using the excluded volume and (b) applying small values of η_2 for the NJL8 quark-matter model. This is illustrated on Fig. 1 where we compare the phase transition constructions from DD2 (blue) and DD2-EV (light blue) to NJL8 (red) with $\eta_2 = 0.08$ and $\eta_4 = 0.0$. The upper panel of Fig. 1 shows pressure vs. chemical potential, from which it becomes clear that our excluded volume approach reduced the critical chemical potential for the onset of quark matter. Furthermore, it also increases the differences between the slopes of the pressure curves for hadronic and quark EoS at the phase transition. The latter aspect results in an increased latent heat, $\Delta\epsilon$, which is shown in the bottom panel of Fig. 1. For the here explored NJL8 parameters ($\eta_2 = 0.08$, $\eta_4 = 0.0$), we find $\Delta\epsilon \simeq 0.34\epsilon_{\text{crit}}$ for the transition with DD2 and $\Delta\epsilon \simeq 0.81\epsilon_{\text{crit}}$ for the transition with DD2-EV.

With the given choice of nuclear matter parameters, the excluded volume correction generates a stiff nuclear EoS at suprasaturation densities, close to the limit of causality, i.e. $c_H^2 \simeq 1$. Furthermore, the choice of small η_4 ensures a soft quark mat-

ter EoS at the phase transition densities, i.e. $c_Q^2 \gtrsim 1/3$. The resulting maximized jump in energy density at the phase transition from DD2-EV to NJL8 is illustrated in Fig. 2 for the parameter range $\eta_4 = 0.0 - 30.0$, for which we obtain $\Delta\epsilon \simeq (0.81 - 0.70)\epsilon_{\text{crit}}$.

Our approach for the construction of a quark-hadron phase transition with large latent heat extends beyond the phenomenological model of Zdunik & Haensel (2013) and Alford et al. (2013), known as ZHAHP. In their approach, the latent heat $\Delta\epsilon$ is a free parameter and the quark EoS is defined by a constant speed of sound c_Q^2 . Nevertheless, in providing as one of the major requirements for the existence of the third family the rule of thumb that the latent heat be around $\Delta\epsilon \simeq 0.6$, the ZHAHP approach proves to be extremely practical (see, e.g., Alvarez-Castillo & Blaschke, 2013). However, it is unphysical treating c_Q^2 and $\Delta\epsilon$ as mutually independent parameters. Within a microscopic description for the EoS both quantities are always correlated, e.g., the relative stiffness of the EoS between hadronic and quark phases defines the latent heat

$$\Delta\epsilon = \mu_B^{\text{crit}} (n_Q - n_H) = (\mu_B^{\text{crit}})^2 \left(c_Q^2 \frac{\partial n_B^Q}{\partial \mu_B} \Big|_{\mu_B^{\text{crit}}} - c_H^2 \frac{\partial n_B^H}{\partial \mu_B} \Big|_{\mu_B^{\text{crit}}} \right). \quad (19)$$

In the above formula all the quantities are evaluated at the critical chemical potential of the transition $\mu_B = \mu_B^{\text{crit}}$.

3.2. Mass-radius relationship

Based on our novel quark-hadron hybrid EoS we calculate the mass-radius relations from solutions of the Tolman-Oppenheimer-Volkoff (TOV) equations. For a selection of quark matter parameters, i.e. constant $\eta_2 = 0.08$ and varying $\eta_4 = 0.0 - 30.0$, we show the resulting mass-radius curves in Fig. 3. Horizontal colored bands mark the constraints from high-precision mass measurements of the high-mass pulsars PSR J1614-2230 and PSR J0348+0432 by Demorest et al. (2010) and Antoniadis et al. (2013), respectively. In Fig. 3, the green shaded vertical bands mark the results of the mass-radius analysis of the millisecond pulsar PSR J0437-4715 by Bogdanov (2013), with 1σ , 2σ and 3σ confidence level assuming a mass of $1.76 M_\odot$. These data form the basis of a new Bayesian analysis of constraints for hybrid EoS parametrizations Alvarez-Castillo et al. (2014) which ought to supersede the first study of this kind by Steiner et al. (2010). In addition, we show data from the X-ray spin phase-resolved spectroscopic study of the thermally emitting isolated neutron star RX J1856.5-3754 by Hambaryan et al. (2014), indicating potential compactness constraints. The solid brown line in Fig. 3 corresponds to the purely hadronic EoS DD2, i.e. without excluded volume corrections, for comparison with DD2-EV.

The here introduced excluded volume approach results in large neutron star radii, $R \simeq 14.75 \text{ km}$ for $M = 1.5 M_\odot$ in comparison to DD2 ($R \simeq 13 \text{ km}$). It can be understood in terms of the significant stiffening of the nuclear EoS above saturation density ($n_{\text{sat}} = 0.149 \text{ fm}^{-3}$). At the phase transition the stellar configuration leaves the stable hadronic branch onto an unstable branch, marked by dotted lines in Fig. 3. The mass-radius coordinates where this happens are defined by the critical chemical potential μ_B^{crit} , or density n_B^{crit} , of the corresponding hybrid EoS. Note that for all hybrid EoS explored in this study, the critical density is $n_B^{\text{crit}} \simeq 1.5n_{\text{sat}}$. More in detail, the initially stable hadronic configuration at μ_B^{crit} grows by a tiny amount of mass ($\sim 5 \times 10^{-4} M_\odot$) while the radius remains constant, into a still stable hybrid branch. We estimate the size of the resulting quark

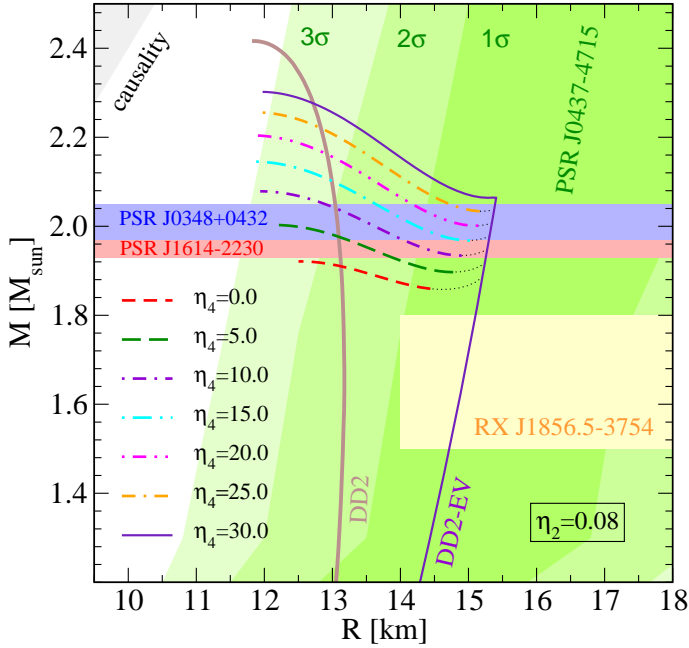


Fig. 3. (Color online) Mass-radius relations for our hybrid DD2-EV NJL8 EoS for constant $\eta_2 = 0.08$ and varying $\eta_4 = 0.0 - 30.0$. Horizontal color bands mark the current $2 M_\odot$ constraints from high-precision mass measurement of high-mass pulsars, PSR J1614–2230 (red) by Demorest et al. (2010) and PSR J0348+0432 (blue) by Antoniadis et al. (2013). For comparison with DD2-EV, the mass-radius curve for the hadronic EoS DD2 is shown in addition (solid brown line). Furthermore, we show results from the mass-radius analysis of the millisecond pulsar PSR J0437–4715 by Bogdanov (2013), and constraints from the X-ray spectroscopic study of the thermally emitting isolated neutron star RX J1856.5–3754 by Hambaryan et al. (2014).

core to be ~ 80 cm with significantly increased density. Only after that, the configuration turns to the unstable branch during which the quark core grows. The unstable branch recovers back to another stable branch due to the strong repulsive force 8-quark interaction of the NJL8 EoS at high densities.

Our selection of nuclear and quark matter parameters allows not only for high mass hadronic and quark configurations, in agreement with the $2 M_\odot$ pulsar data from Demorest et al. (2010) and Antoniadis et al. (2013), but also for the consistent transition from the hadronic branch to the quark-hadron hybrid branch. Here we identify the latter as the third-family of compact stellar objects, with maximum masses in the range $M_{\max} = 1.92 - 2.30 M_\odot$ which are above those of the underlying hadronic model DD2-EV. Moreover, we confirm that all hybrid EoS fulfill the condition of causality, i.e. the maximum speed of sound of the hybrid star configurations is in the range $c_Q^2 = 0.34 - 0.82$. In addition, our results are in agreement with the mass-radius analysis of the millisecond pulsar PSR J0437–4715 by Bogdanov (2013) within 3σ confidence level (see the green vertical bands in Fig. 3), as well as with the compactness study of the isolated neutron star RX J1856.5–3754 by Hambaryan et al. (2014) (see the yellow box in Fig. 3) where radius of around 14–18 km at a mass range of $1.5 - 1.8 M_\odot$ were found within the 1σ confidence level (see also Trümper, 2011).

3.3. Radii difference of the high-mass twins

The most striking consequence of a strong first order phase transition in compact star matter is the possible existence of a third family of compact stars, a branch of stable hybrid star configurations in the mass-radius diagram disconnected from the second family branch of ordinary hadronic stars entailing the twin phenomenon: for a certain range of masses there exist pairs of stars (twins) with the same gravitational mass but different internal structure. In order to quantify the unlikeness of the twins as a measure of the pronouncedness of the phase transition we consider the radii difference $\delta R = R_{\max} - R_{\text{twin}}$ between the radius at the maximum mass M_{\max} on the hadronic branch and that of the corresponding mass twin on the third family branch of hybrid star configurations. In Table 2, we list δR at fixed $\eta_2 = 0.08$ for selected values of the dimensionless eight-quark interaction strength η_4 in the range where it allows for the twin phenomenon (see also Fig. 3 for comparison).

Table 2. Parameters of high-mass twin neutron star configurations for the relevant range of dimensionless eight-quark interaction couplings η_4 in the vector meson channel at fixed $\eta_2 = 0.08$. For details see text.

η_4	M_{\max} [M_\odot]	R_{\max} [km]	R_{twin} [km]	δR [km]	$\Delta\varepsilon$ [ϵ_{crit}]
0.0	1.89	15.21	13.61	1.59	0.81
5.0	1.92	15.24	14.09	1.16	0.79
10.0	1.95	15.28	14.27	0.91	0.77
15.0	1.98	15.31	14.61	0.70	0.75
20.0	2.01	15.34	14.82	0.52	0.73
25.0	2.04	15.38	15.01	0.36	0.72
30.0	2.07	15.36	15.23	0.13	0.70

The largest radii difference we obtain for $\eta_4 = 0.0$, however, for M below the current maximum mass constraint of Demorest et al. (2010) and Antoniadis et al. (2013). In agreement with these latter constraints are the parametrizations $\eta_4 = 5.0 - 30.0$, with $\delta R = 1.16 - 0.13$ km. The reduced radii difference for increasing η_4 can be understood not only from the stiffening of the quark matter EoS at high densities but also from the reduced latent heat $\Delta\varepsilon$, i.e. the reduced jump in energy density going from the hadronic EoS to the hybrid EoS (see Fig. 2), also listed in Table 2. From the required condition $\Delta\varepsilon > 0.6\epsilon_{\text{crit}}$, it becomes clear from Table 2 that twin configurations are only obtained for $\eta_4 = 0.0 - 30.0$. For $\eta_4 \gtrsim 30.0$ the phase transition to quark matter proceeds without developing a disconnected third family branch - all configurations on this sequence up to the maximum mass are stable (see also Fig. 3).

4. Conclusions

Compact stars harbor central densities in excess of nuclear saturation density, conditions which are currently inaccessible in nuclear high-energy experiments. Their study contributes to a key direction of research in nuclear and hadron physics, i.e. the possible transition from a state of matter with nuclear degrees of freedom to a deconfined state with quark and gluon degrees of freedom. Despite the success of lattice QCD at vanishing chemical potential and high temperatures identifying the nature of the transition as crossover, for finite chemical potentials only phenomenological models can be used (c.f. Lattimer & Prakash, 2010; Klähn et al., 2013; Buballa et al.,

2014, and references therein). Such models, in particular with the phase transition from nuclear to quark matter, have been very useful also in astrophysical application, e.g., in simulations of protoneutron star cooling (c.f. Pons et al. , 2001; Popov et al. , 2006; Blaschke et al. , 2013) and simulations of core-collapse supernovae (c.f. Sagert et al. , 2009; Fischer et al. , 2011; Nakazato et al. , 2014). It is therefore of paramount interest to develop quark-hadron hybrid models from which it is possible to deduce observables that allow us to further constrain the yet highly uncertain QCD phase diagram, e.g., the possible existence of a critical point. Such identification will be possible with the discovery of a first-order phase transition at low temperatures and large chemical potential, conditions which refer to the state of matter at compact star interiors in β -equilibrium.

In this paper, we took on this challenge and developed a novel quark-hadron hybrid EoS. It is based on the nuclear EoS DD2, which is a relativistic mean-field model with density-dependent couplings. While such models treat nucleons as point-like quasi-particles, here we take in addition finite size effects of the nucleons into account via an excluded-volume approach above nuclear saturation density. The excluded volume correction introduced here is an attempt to account for the Pauli blocking at the quark level. However, at the current status it is still quite basic and will be improved in an upcoming study. For the quark matter EoS we apply the NJL model formalism, including higher order repulsive quark interactions. The latter become dominant in particular at high densities. Note that the current status of research for the vector interactions in quark matter remains unsettled (for details, see e.g. Steinheimer & Schramm , 2014; Sugano et al. , 2014) and its impact on the possible existence of the CEP remains an open question (see Bratovic et al. , 2013; Contrera et al. , 2014; Hell et al. , 2013, and references therein). The quark-hadron phase transition has been constructed applying the Maxwell criterion, which results in a strong first-order phase transition. The excluded volume on the hadronic side, in combination with the stiff quark EoS, results in not only in an early onset of quark matter but also in a large latent heat at the phase transition.

From our novel hybrid EoS which we provide to the community for different values of the higher order quark interaction strength, we have constructed the mass-radius relations based on TOV solutions. Our main findings can be summarized as follows:

- (1) The excluded volume for the high-density nuclear EoS results in large radii for intermediate-mass neutron stars.
- (2) The transition to quark matter results in a *first* stable hybrid configuration with tiny quark core, which then turns to the unstable branch.
- (3) The unstable branch recovers back to a stable hybrid branch due to the strong repulsive higher-order quark interactions, which we identify as *third family* of compact stars

For all configurations explored in this study, we find that the maximum masses belong to the stable hybrid branch and that all EoS remain causal. Moreover, most of our parameter choices fulfil a variety of current constraints on mass-radius relations, such as large maximum masses around $2 M_{\odot}$ (Demorest et al. , 2010; Antoniadis et al. , 2013) and radii in the range of 14–17 km for canonical compact objects of $M \approx 1.7 M_{\odot}$ (Bogdanov , 2013; Hambaryan et al. , 2014).

From an observational perspective, a particularly interesting consequence of a third family of compact objects is the twin

phenomenon, where two stars of the same mass have different radii. In the present paper, we even found high-mass twins with $M \approx 2 M_{\odot}$ with radius differences on the order of about 1 km. It remains to be shown whether future surveys that are devoted to neutron star radii determinations, such as the X-ray satellite missions NICER, SKA and NUSTAR, will have the required sensitivity of less than 1 km, in order to resolve the twin phenomenon. It would, in turn, provide a unique signature of a first-order phase transition to exotic superdense matter in compact star interiors.

The aspects discussed in this paper may have important consequences when taken into account consistently in dynamical simulations of supernova collapse and explosions, binary mergers and so on, where during the phase transition the gain in gravitational binding energy will be available to the system as heat, which in turn can trigger the local production of neutrinos due to the different β -equilibrium condition obtained. Furthermore, the current work improves on the previous phenomenological studies of Alford et al. (2013) and Alvarez-Castillo & Blaschke (2013), where the latent heat and the speed of sound were considered as mutually independent parameters.

Acknowledgements

We gratefully acknowledge numerous discussions and collaboration work on the topic addressed in this contribution with our colleagues, in particular with A. Ayriyan, G. A. Contrera, H. Grigorian, O. Kaczmarek, T. Klähn, E. Laermann, R. Lastowiecki, M. C. Miller, G. Poghosyan, S. B. Popov, M. Sokolowski, J. Trümper, D. N. Voskresensky and F. Weber. This research has been supported by Narodowe Centrum Nauki within the “Maestro” programme under contract number DEC-2011/02/A/ST2/00306. The visits of S. B. and D. E. A.-C. at the University of Wrocław were supported by the COST Action MP1304 “NewCompStar” within the STSM programme. S. B. acknowledges partial support by the Croatian Science Foundation under Project No. 8799. D. B. acknowledges support by the Polish Ministry for Science and Higher Education under grant number 1009/S/IFT/14. D. E. A.-C. is grateful for support by the Heisenberg-Landau programme for collaboration between JINR Dubna and German Universities and Institutes. S. T. acknowledges support by the Helmholtz Association (HGF) through the Nuclear Astrophysics Virtual Institute (VH-VI-417), and by the Heisenberg-Landau programme.

References

- Agrawal, B. K., & Dhiman, S. K. 2009, Phys. Rev. D **79**, 103006
 Agrawal, B. K. 2010, Phys. Rev. D **81**, 023009
 Akmal, A., Pandharipande, V. R., Ravenhall, D. G., 1998, Phys. Rev. C **58**, 1804
 Alford, M., Braby, M., Paris, M. W. & Reddy, S. 2005, Astrophys. J. **629**, 969
 Alford, M. G., Han, S., & Prakash, M. 2013, Phys. Rev. D **88**, 083013
 Alvarez-Castillo, D., Ayriyan, A., Blaschke, D. & Grigorian, H. 2014, arXiv:1408.4449 [astro-ph.HE]
 Alvarez-Castillo, D. E., & Blaschke, D. 2013, *Proving the CEP with compact stars?*, Proc. of 17th Conference of Young Scientists and Specialists, Dubna, April 8-12, 2013, pp 22 - 26; arXiv:1304.7758 [astro-ph.HE]
 Antoniadis, J., et al. 2013, Science **340**, 6131
 Banik, S., & Bandyopadhyay, D. 2001, Phys. Rev. C **64**, 055805
 Banik, S., & Bandyopadhyay, D. 2003, Phys. Rev. D **67**, 123003
 Benić, S. 2014, Eur. Phys. J. A **50**, 111
 Blaschke, D., Alvarez-Castillo, D. E., & Benić, S. 2013, PoS **CPOD 2013**, 063
 Blaschke, D., Grigorian, H. & Voskresensky, D. N., 2013, Phys. Rev. C **88**, 065805
 Bogdanov, S. 2013, Astrophys. J. **762**, 96
 Bratovic, N., Hatsuda, T., & Weise, W. 2013, Phys. Lett. B **719**, 131
 Buballa, M., Dexheimer, V., Drago, A., et al. 2014, arXiv:1402.6911
 Contrera, G. A., Grunfeld, A. G., Blaschke, D. B. 2014, Phys. Part. Nucl. Lett., **11**, 342

- Demorest, P., et al. 2010, *Nature* **467**, 1081
- Fischer, T., Sagert, I., Pagliara, G., Hempel, M., Schaffner-Bielich, J., Rauscher, T., Thielemann, F.-K.; Käppeli, R.; Martínez-Pinedo, G. & Liebendörfer, M., 2011, *Astrophys. J. Suppl.* **194**, 28
- Fraga, E. S., Pisarski, R. D., & Schaffner-Bielich, J. 2002, *Nucl. Phys. A* **702**, 217
- Fraga, E. S., Kurkela, A., & Vuorinen, A. 2014, *Astrophys. J. Lett.* **781**, L25
- Fuchs, C., 2006, *Prog. Part. Nucl. Phys.* **56**, 1
- Fukushima, K., & Sasaki, C. 2013, *Prog. Part. Nucl. Phys.* **72**, 99
- Fukushima, K. 2014, arXiv:1408.0547
- Gendreau K. C., et al. 2012, *Proc. SPIE Space Telescopes and Instrumentation*, 8443, 844313
- Gerlach, U. H. 1968, *Phys. Rev.* **172**, 1325
- Glendenning, N. K., & Kettner, C. 2000, *Astron. Astrophys.* **353**, 795
- Haensel, P., Potekhin, A. Y., & Yakovlev, D. G. 2007, *Neutron stars 1: Equation of state and structure*, Springer, Heidelberg
- Hambaryan, V., Neuhäuser, R., Suleimanov, V., & Werner, K. 2014, *J. Phys. Conf. Ser.* **496**, 012015.
- Hebeler, K., Lattimer, J. M., Pethick, C. J., & Schwenk, A. 2013, *Astrophys. J.* **773**, 11
- Hell, T., Kashiwa, K., & Weise, W. 2013, *J. Mod. Phys.* **4**, 644
- Inoue, T., Aoki, S., Doi, T., et al. 2013, *Phys. Rev. Lett.* **111**, 112503
- Kämpfer, B. 1981, *J. Phys. A* **14**, L471
- Kashiwa, K., Kouno, H., Sakaguchi, T., Matsuzaki, M., & Yahiro, M. 2007, *Phys. Lett. B* **647**, 446
- Klähn, T., Blaschke, D., Sandin, F., Fuchs, C., Faessler, A., Grigorian, H., Röpke, G. and Trümper, S. 2007, *Phys. Lett. B* **654**, 170
- Klähn, T., Łastowiecki, R., & Blaschke, D. 2013, *Phys. Rev. D* **88**, 085001
- Lattimer, J. M., & Prakash, M. 2010, arXiv:1012.3208
- Masuda, K., Hatsuda, T., & Takatsuka, T., 2013, *Prog. Theor. Phys.* **2013**, 073D01
- Mignani, R. P., et al. 2012, *IAU Symposium*, 285, 372 ; arXiv:1201.0721
- Miller, M. C. 2013, arXiv:1312.0029
- Nakazato, K., Sumiyoshi, K. & Yamada, S. 2014 , *Astronom. Astrophys.* **558**, 5
- Ohnishi, A., Ueda, H., Nakano, T., Ruggieri, M., Sumiyoshi, K. 2011, *Phys. Lett. B* **704**, 284
- Orsaria, M., Rodrigues, H., Weber, F., & Contrera, G. A. 2013, *Phys. Rev. D* **87**, 023001
- Pons, J. A., Steiner, A. W., Prakash, M., & Lattimer, J. M. 2001, *Phys. Rev. Lett.* **86**, 5223
- Popov, S. B., Grigorian, H., & Blaschke, D. 2006, *Phys. Rev. C* **74**, 025803
- Read, J. S., Lackey, B. D., Owen, B. J., & Friedman, J. L. 2009, *Phys. Rev. D* **79**, 124032
- Rischke D. H., Gorenstein M. I., Stoecker H., & Greiner W. 1991, *Z. Phys. C* **51**, 485
- Sagert, I., Fischer, T., Hempel, M., Pagliara, G., Schaffner-Bielich, J., Mezzacappa, A., Thielemann, F.-K. & Liebendörfer, M. 2009, *Phys. Rev. Lett.* **102**, 081101
- Schaffner-Bielich, J., Hanauske, M., Stöcker, H., & Greiner, W. 2002, *Phys. Rev. Lett.* **89**, 171101.
- Schertler, K., Greiner, C., Schaffner-Bielich, J., & Thoma, M. H. 2000, *Nucl. Phys. A* **677**, 463
- Steiner, A. W., Lattimer, J. M., & Brown, E. F. 2010, *Astrophys. J.* **722**, 33
- Steiner, A. W., Lattimer, J. M., & Brown, E. F. 2013, *Astrophys. J.* **765**, L5
- Steinheimer, J., & Schramm, S. 2014, *Phys. Lett. B* **736**, 241
- Sugano, J., Takahashi, J., Ishii, M., Kouno, H., & Yahiro, M. 2014, *Phys. Rev. D* **90**, 037901
- Trümper, J. E. 2011, *Prog. Part. Nucl. Phys.* **66**, 674
- Typel, S., & Wolter, H. H. 1999, *Nucl. Phys. A* **656**, 331
- Typel, S., Röpke, G., Klähn, T., Blaschke, D., & Wolter, H. H. 2010, *Phys. Rev. C* **81**, 015803
- Yamamoto, Y., Furumoto, T., Yasutake, N., & Rijken, T. A. 2014, arXiv:1406.4332
- Yasutake, N., Łastowiecki, R., Benić, S., Blaschke, D., Maruyama, T., & Tatsumi, T. 2014, *Phys. Rev. C* **89**, 065803
- Zdunik, J. L., & Haensel, P. 2013, *Astron. Astrophys.* **551**, A61